Quantifying metasomatic HFSE-REE transport from alkaline magmas

Krzysztof Sokół[1]*, Adrian A. Finch[1], William Hutchison[1], Jonathan Cloutier[1,2], Anouk M. Borst[1,3,4], Madeleine C. S. Humphreys[5]

[1] *School of Earth and Environmental Sciences, University of St Andrews, St Andrews, KY16 9TS, UK*

[2] *Centre for Ore Deposit and Earth Sciences (CODES), University of Tasmania, Hobart TAS 7001*

[3] *Dept of Earth and Environmental Sciences, KU Leuven, 3001 Heverlee, Belgium*

[4] *Dept of Geodynamics and Mineral Resources, Royal Museum for Central Africa, B-3080 Tervuren, Belgium*

[5] *Dept of Earth Sciences, Durham University, Durham, DH1 3LE, UK*

** Corresponding author email: ks275@st-andrews.ac.uk*

ABSTRACT

Alkaline igneous rocks host many global High Field Strength (HFSE) and Rare Earth Element (REE) deposits. While HFSE are commonly assumed to be immobile in hydrothermal systems, transport by late-stage hydrothermal fluids associated with alkaline magmas is reported. However the magnitude of the flux and the conditions are poorly constrained and essential to understanding the formation of REE-HFSE ores. Here we examine the alteration of country rocks ('fenitization') accompanying the emplacement of a syenite magma at Illerfissalik in Greenland, through analysis of changes in rock chemistry, mineralogy and texture. Our novel geochemical maps show a 400 m wide intrusion aureole, within which we observe typically tenfold increases in the concentrations of many elements, including HFSE. Textures suggest both pervasive and structurally-hosted fluid flow, with initial reaction with the protolith's quartz cement leading to increased permeability and enhancing chemical interaction with a mixed Ca-K-Na fenitizing fluid. We estimate the HFSE masses transferred from the syenite to the fenite by this fluid and find ~43 Mt of REE were mobilised (~12% of the syenite-fenite system TREO budget) – a mass comparable to the tonnages of some of the world's largest HFSE resources. We argue that fenite can yield crucial information about the tipping points in magma evolution as retention or loss of volatile-bonded alkali and HFSE is key for development of magmatic zirconosilicate-hosted HFSE ores (i.e. Kringlerne, Ilimaussaq), or formation of the syenite-hosted Nb-Ta-REE (Motzfeldt-type) roof-zone deposits.

Keywords: fenite, mass-transfer, critical elements, alkaline magmas, rare-earth-elements, skarn

INTRODUCTION

The global shift towards low-carbon, hi-tech lifestyles requires better understanding of the petrogenesis of alkaline igneous critical metal deposits. These host many of the world's high-field strength (HFSE) and rare-earth elements (REE; Goodenough et al., 2018) essential to the material production chain e.g. alloys, batteries, magnets and superconductors (European Commission, 2020). The assumption that HFSE are immobile in natural geological systems is valid in most crustal settings (Kranidiotis & MacLean, 1987; Hastie et al., 2007), but at variance with a body of evidence that HFSE are mobile in fluids associated with mineralized carbonatite and alkaline-silicate magmas. Alkaline igneous hosted HFSE mineral deposits are of two types: 1) roof zone-related HFSE-deposits, where fluid-rich alkaline magma interacts with a roof (Finch et al., 2019), and 2) highly evolved, persodic, volatile-rich 'agpaitic' magmas where prolonged fractionation crystallizes HFSE-rich magmatic minerals i.e. eudialyte (Marks & Markl, 2017). Alkaline magmas in the upper crust often expel a high-temperature fluid phase that modifies the country rock envelope ("fenitization"; Elliott et al., 2018) and the source intrusions ("autometasomatism"; Salvi & Williams-Jones, 1996; van de Ven et al., 2019). The alteration haloes ('fenite zones') are rarely reported to be wider than 100 m, but the spatial variations of fenitization are often poorly constrained, and several exceptions have been identified i.e. Iivaara (Sindern & Kramm, 2000). A key gap in our understanding is the nature of the fenitizing fluid, the magnitude of chemical exchange and the relationships between fenite and ore deposits.

This study examines a fenite in the Mesoproterozoic Gardar alkaline Province, SW Greenland, superbly exposed due to recent glaciation. The fenite formed adjacent to the Illerfissalik nepheline syenite centre (Fig. 1A-1B) replacing laterally homogeneous quartz arenite country rock. Whole-rock geochemistry supported by detailed textural and mineralogical observations allow us to fingerprint the composition of the fluid and estimate the magnitude of element exchange between fluid and host rock. We calculate the REE and HFSE tonnage transported from the magmatic hearth into the wall-rocks showing that fenitization is significant to HFSE-REE resource formation, and explore its role in alkaline magma evolution. This approach provides key insights into the genesis of globally significant HFSE deposits.

GEOLOGICAL SETTING

The regional basement of SW Greenland comprises Paleoproterozoic granitoids (1.8 Ga; Garde et al., 2002) formed at an Andean-type continental margin during assembly of the Nuna/Columbia supercontinent (Meert & Santosh, 2017). Rifting at 1.3 Ga formed the 'Gardar

Province' (ca. 1.32-1.14 Ga; Upton, 2013), which began by deposition of a 3-3.5 km thick interbedded sequence of rift-related sedimentary-volcanic rocks (the Eriksfjord Group) onto the basement (1.3 Ga; Piper et al., 1999). Regional NE-SW trending dykes (i.e. the Igaliko Dyke-Swarm; Pearce, 1988) then cut both the basement and the Eriksfjord Group. Finally, syenite magmas of the Illerfissalik centre (c. 1.14 Ga; Upton, 2013) intruded this sequence forming shallow (100-200 MPa; Konnerup-Madsen & Rose-Hansen, 1984) nested, subvolcanic systems (Emeleus & Harry, 1970; Fig. 1A-1B), cut occasionally by the last of the regional dykes and the small syenite-hosted NYF-like (cf. Goodenough et al., 2019) Narsaarsuk and Nanna pegmatites. Fluids from Illerfissalik fenitized the Eriksfjord to the west and the older syenites to the north and east (Finch, 1995).

SAMPLING AND ANALYTICAL METHODS

Fieldwork took place in a ~6 km^2 area of fenitization at the contact between the Illerfissalik I4 augite syenite and the basal Eriksfjord Group (Fig. 1A-1B) at the S bank of Tunulliarfik Fjord. We document the geological (Fig. 1D-1E) and geochemical expression as a function of distance from Illerfissalik and undertake petrography (optical microscopy, SEM , i.e. Fig. DR1.1, and semi-quantitative energy-dispersive-spectroscopy – EDS) to identify secondary minerals. Major and trace element whole-rock data are presented for 39 fenite, 15 unaltered Eriksfjord and nine I4 syenite samples. Supplementary Material (Text DR1 & Tables DR2) contains detailed information on analytical methods, data and accuracy & precision (Table DR1.2 for standardization summary).

DESCRIPTION AND QUANTIFICATION OF FENITIZATION

The unaltered Eriksfjord host rocks are white to red (hematite dusting; Fig. 1C), mature quartz arenite (<5% modal K-feldspar) deposited in a braided fluvio-aeolian environment (Piper et al., 1999). Fenite which formed from alteration of the Eriksfjord is pale in colour comprising corroded quartz, with secondary patch-perthite and Ca and Na-Ca mafic minerals defining podiform sub-planar domains (i.e. Fig. 1D-1E; DR1.1B) by replacement of silica cement (Fig. DR1.1A) and Ca-rich amphibole cores often thinly rimmed by Na end-members (Fig. DR1.1E,G). Other minerals introduced by fenitization are HFSE-bearing titanite, zircon, chevkinite-group minerals and the Mn-phosphate dickinsonite (in hematite-rich fenite). Fenite is mappable up to ~400 m from the contact, beyond which thermally indurated quartz arenite is typically observed. More detail on scale and intensity of alteration is provided in Supplement DR1.

Using our whole-rock dataset, we quantify element mass-transfer by applying the Grant (1986) model in a 'constant mass' (CM) scenario (Kresten, 1988) using the EASYGRESGRANT program (López-Moro, 2012; see Supplementary Material for full parameters). We use an average composition of the Eriksfjord arenite (n=15, Fig. 2A) as a baseline for reconstructing the relative mobility of elements in the fenite zone. We focus on N and S portions of the fenite (Fig. 2B, 2C) and a dyke margin at Illiortarfik ~1.2 km from the contact (Fig. 2D). Several elements show no apparent deviation from the mean protolith composition due to metasomatism (SiO_2, Ta – Fig. 2B; SiO_2, Zr, Y, Tm - Fig. 2C; SiO_2, K_2O, Cr – Fig. 2D), however petrographic evidence suggests most are at least locally mobile (Fig. DR1.1). Estimates of the volume (f_v) necessary to preserve constant mass (see Fig. DR1.2 and the Supplementary text for more detail) suggest a maximum volume change <~20% (blue lines in Fig. 2), assuming density of altered and unaltered rocks is 2.6-2.8 g/cm^3 (Text DR1, Table DR1.3).

Grant's calculated change parameter (ΔC_i,) is divided by the original concentration ($\Delta C_i/C_i^O$) to quantify the chemical alteration. Spatial interpolation of this parameter across the field area shows a sharp alteration boundary at ~400 m distance, particularly in the north where enrichment in Ca, Na, K and Ti (high $\Delta C_i/C_i^O$ values; Fig. 3A-3D) and higher ΣLREE/ΣHREE are observed (Fig. 3E). HFSE are broadly higher towards the contact (Fig. 3D-3F), but excursions in $\Delta C_{Ti}/C_{Ti}^O$ and log(ΣZr-Nb-Ta) (Fig. 3F) occur at distance (U-Th also correlating with ~100x gain - see Table DR2.1 in Data Repository) along contacts with Igaliku dykes (IDS; Fig. 1B, Fig. 3) at Illiortarfik ~1.3 km from the syenite, often correlating with $\Delta C_{Na}/C_{Na}^O$ (Fig. 3A, 3D).

Based on geochemical and microtextural evidence (Fig. DR1.1), we infer that the metasomatic changes were caused by a hot (>600°C) orthomagmatic Ca-K-Na-bearing fluid. Petrography indicates that metasomatism began with SiO_2-cement dissolution, which we attribute to the HF-driven reaction triggered by the F-rich Illerfissalik late-stage fluids (Finch, 1995). Some experimental studies discussing geochemically similar granitic fluids (cf. Lundstrom, 2020) suggest such a fluid phase may be volatile-rich and others indicate F may strongly partition into this fluid exsolving from a phonolite magma at 800°C and 200 MPa (Chevychelov et al., 2008). Presence of secondary titanite instead of fluorite may also suggest the fluid is hot (>500°C), HFSE, alkali and volatile-rich (Scaillet & Macdonald, 2004). Upon separation from the magma, the Ca-K-Na fluid leaches silica and is then free to penetrate the country rock matrix pervasively. The resultant alteration is metaluminous (i.e. molecular

$\frac{(Ca+Na+K)}{Al} > 1$, but $\frac{(Na+K)}{Al} < 1$), strongly resembling other syenite-related fenites (Borralan, Scotland; Iivaara, Finland; Woolley et al., 1972; Sindern & Kramm, 2000), but gain in alkalis and Ca (to a lesser degree) also occurs where carbonatite is present or dominant (i.e. Alnö, Amba Dongar, Vishnevye Mts, see Abramov et al., 2020; Elliott et al., 2018 and references therein). Our novel spatial visualization (Fig.3A-D) showcases the chemical footprint of fluid emanating from a strictly alkaline-silicate magma forming a laterally extensive fenite, until now best detected by geophysics in areas of poor exposure (i.e. Alnö; Yan et al., 2016). The narrow Na-rich rims upon Na-Ca amphiboles (Fig. DR1.1E) within the aureole indicate either the evolving chemistry of fluids, or subsequent overprint by a separate dominantly sodic pulse and may suggest it was comparatively low in volume to the early-stage Ca-K-Na event. Na enrichment often correlates with HFSE-Ti (Fig. 2D, 3A, 3D, 3F), and the distribution of fenite at distance (usually next to regional dykes) may suggest fracture-assisted flow occurring together with pervasive fenitization. Precipitation of secondary Zr-Nb-Ti-LREE-rich minerals, only visible in thin-section (Fig. DR1.1), may be controlled locally by gradients in temperature and/or chemistry (Akinfiev et al., 2020).

IMPLICATIONS FOR MINERALISATION AND PROSPECTIVITY

Assuming the wall-rock and intrusion are homogeneous and that the fenite forms a uniform carapace around the intrusion, we perform a geometry-based (Fig. DR1.3) estimate of the HFSE mass lost to the wall rocks (detailed steps provided in Supplementary Material). The total HFSEO budget within the Illerfissalik system [$HFSEO_{Total} = HFSEO_{intrusion} + (HFSEO_{fenite} – HFSEO_{protolith})$], excluding TiO_2, is ~801 Mt (Table DR2.2). Of this, ~62 Mt of HFSEO was flushed into the country rocks, of which ~43 Mt are TREO (Table DR2.2) and this mass accounts for ~12% of the $TREO_{Total}$ budget in the Illerfissalik syenite/fenite system, consistent with the presence of newly formed HFS- and REE-bearing minerals (Table DR1.1). Although all HFSE are enriched in fenite relative to the protolith, Nb_2O_5 and LREO are the highest (~1 order of magnitude; Fig. 4A). Strikingly, the estimates of masses transported into the fenite are comparable to the tonnage of world-class ore deposits (e.g. Kringlerne, held by Tanbreez A/S: 31 Mt TREO, Fig. 4B; Zhou et al., 2017) and highlight the exceptional capability of fenitizing fluids as commodity carriers.

Illerfissalik allows one to draw key inferences for the genesis of HFSE mineral deposits in alkaline systems. The prevalence of calc-silicates in the aureole (Fig. 1D, 1E; DR1.1) and the mixed Ca-K-Na fluid nature (Fig. 2B, 2C) suggest a skarn-like (garnet-absent) high-temperature process reminiscent of ‘antiskarn’ alteration whereby REE-Th ores develop in diopside-selvaged fractures within carbonate-free wall-rocks (Anenburg & Mavrogenes, 2018). Although carbonatites are present in the region (Pearce, 1988), Ca may come from a) the overlying Ca-rich wall-rock by circulating hydrothermal fluids (Salvi & Williams-Jones, 1996), b) fluid mixing with seawater (Graser & Markl, 2008) or c) Ca redistribution from magmatic phases of the source intrusion – the last of which we find most plausible in this case. Similar processes, but acting in stoped roof zones characterize syenite-hosted Nb-Ta-REE mineralization (e.g. Finch et al., 2019). Finally, the wall-rock permeability is critical for understanding the evolution of large, shallow intrusions like Illerfissalik surrounded by what likely was a relatively hot immediate crust promoting significant outgassing (Parmigiani et al., 2017). Loss of volatiles together with ~12% of the REE and the alkali to the fenite may have impacted the magma evolution towards a Na-HFSE-rich, eudialyte-bearing composition (Marks et al., 2011). These findings highlight the similarities between skarn systems and the long-neglected fenitization process – a phenomenon crucial to our understanding of HFSE ore genesis.

ACKNOWLEDGMENTS

This work was supported by NERC IAPETUS DTP (ref: NE/L002590/1). A.A.F., W.H. and A.M.B. acknowledge support from the SoS RARE (ref: NE/M010856/1) and HiTech AlkCarb consortia of the EU Horizon 2020 R&I programme – grant 689909; W.H. also acknowledges a UKRI Future Leaders Fellowship (ref: MR/S033505/1). Many thanks to field assistants including L. Spindler, G. Colleran, A. Murphy, L. Mathieson and R. Webster for their tireless work, and to Blue Ice Explorers for reliable logistical support in Greenland. We thank Jerry Dickens who was an efficient science editor and the four anonymous reviewers whose comments greatly improved this manuscript.

REFERENCES CITED

Abramov, S.S., Rass, I.T., and Kononkova, N.N., 2020, Fenites of the Miaskite–Carbonatite Complex in the Vishnevye Mountains, Southern Urals, Russia: Origin of the Metasomatic Zoning and Thermodynamic Simulations of the Processes: Petrology, v. 28, p. 263–286, doi:10.1134/S0869591120030029.

Akinfiev, N.N., Korzhinskaya, V.S., Kotova, N.P., Redkin, A.F., and Zotov, A. v, 2020, Niobium and tantalum in hydrothermal fluids: Thermodynamic description of hydroxide and hydroxofluoride complexes: Geochimica et Cosmochimica Acta, v. 280, p. 102–115, doi:10.1016/j.gca.2020.04.009.

Anenburg, M., and Mavrogenes, J.A., 2018, Carbonatitic versus hydrothermal origin for fluorapatite REE-Th deposits: Experimental study of REE transport and crustal "Antiskarn" metasomatism: American Journal of Science, v. 318, p. 335–366, doi:10.2475/03.2018.03.

Chevychelov, V.Yu., Botcharnikov, R.E., and Holtz, F., 2008, Partitioning of Cl and F between fluid and hydrous phonolitic melt of Mt. Vesuvius at ~ 850-1000 °C and 200 MPa: Chemical Geology, v. 256, p. 172–184, doi:10.1016/j.chemgeo.2008.06.025.

Elliott, H.A.L., Wall, F., Chakhmouradian, A.R., Siegfried, P.R., Dahlgren, S., Weatherley, S., Finch, A.A., Marks, M.A.W., Dowman, E., and Deady, E., 2018, Fenites associated with carbonatite complexes: A review: Ore Geology Reviews, v. 93, p. 38–59, doi:10.1016/j.oregeorev.2017.12.003.

Emeleus, C.H., and Harry, W.T., 1970, The Igaliko Nepheline Syenite Complex: General Description: Grønlands Geologiske Undersøgelse Bulletin, v. 85, p. 115.

European Commission, 2020, Study on the review of the list of Critical Raw Materials - Final Report: Critical Raw Materials Factsheets, p. 515, doi:10.2873/11619.

Finch, A.A., 1995, Metasomatic overprinting by juvenile igneous fluids, Igdlerfigsalik, South Greenland: Contributions to Mineralogy and Petrology, v. 122, p. 11–24, doi:10.1007/s004100050109.

Finch, A.A., McCreath, J.A., Reekie, C.D.J., Hutchison, W., Ismaila, A., Armour-Brown, A., Andersen, T., and Simonsen, S.L., 2019, From Mantle to Motzfeldt: A genetic model for syenite-hosted Ta,Nb-mineralisation: Ore Geology Reviews, v. 107, p. 402–416, doi:10.1016/j.oregeorev.2019.02.032.

Garde, A.A., Hamilton, M.A., Chadwick, B., Grocott, J., and McCaffrey, K.J.W., 2002, The Ketilidian orogen of South Greenland: geochronology, tectonics, magmatism, and forearc accretion during Palaeoproterozoic oblique convergence: Canadian Journal of Earth Sciences, v. 39, p. 765–793, doi:10.1139/e02-026.

Goodenough, K.M., Shaw, R.A., Smith, M., Estrade, G., Marquis, E., Bernard, C., and Nex, P., 2019, Economic mineralization in pegmatites: Comparing and contrasting NYF and LCT examples: Canadian Mineralogist, v. 57, p. 753–755, doi:10.3749/canmin.AB00013.

Goodenough, K.M., Wall, F., and Merriman, D., 2018, The Rare Earth Elements: Demand, Global Resources, and Challenges for Resourcing Future Generations: Natural Resources Research, v. 27, p. 201–216, doi:10.1007/s11053-017-9336-5.

Grant, J.A., 1986, The Isocon Diagram - A Simple Solution to Gresens' Equation for Metasomatic Alteration: Economic Geology, v. 81, p. 1976–1982.

Graser, G., and Markl, G., 2008, Ca-rich ilvaite-epidote-hydrogarnet endoskarns: A record of late-magmatic fluid influx into the persodic Ilímaussaq complex, South Greenland: Journal of Petrology, v. 49, p. 239–265, doi:10.1093/petrology/egm079.

Hastie, A.R., Kerr, A.C., Pearce, J.A., and Mitchell, S.F., 2007, Classification of Altered Volcanic Island Arc Rocks using Immobile Trace Elements: Development of the Th–Co Discrimination Diagram: Journal of Petrology, v. 48, p. 2341–2357, doi:10.1093/petrology/egm062.

Konnerup-Madsen, J., and Rose-Hansen, J., 1984, Composition and significance of fluid inclusions in the Ilímaussaq peralkaline granite, South Greenland: Bulletin de Minéralogie, v. 107, p. 317–326, doi:10.3406/bulmi.1984.7761.

Kranidiotis, P., and MacLean, W.H., 1987, Systematics of chlorite alteration at the Phelps Dodge massive sulfide deposit, Matagami, Quebec: Economic Geology, v. 82, p. 1898–1911, doi:10.2113/gsecongeo.82.7.1898.

Kresten, P., 1988, The chemistry of fenitization: Examples from Fen, Norway: Chemical Geology, v. 68, p. 329–349, doi:10.1016/0009-2541(88)90030-7.

Ladenburger, S., Marks, M.A.W., Upton, B.G.J., Hill, P., Wenzel, T., and Markl, G., 2016, Compositional variation of apatite from rift-related alkaline igneous rocks of the Gardar Province, South Greenland: American Mineralogist, v. 101, p. 612–626, doi:10.2138/am-2016-5443.

López-Moro, F.J., 2012, EASYGRESGRANT—A Microsoft Excel spreadsheet to quantify volume changes and to perform mass-balance modeling in metasomatic systems: Computers and Geosciences, v. 39, p. 191–196, doi:10.1016/j.cageo.2011.07.014.

Lundstrom, C.C., 2020, Continuously Changing Quartz-Albite Saturated Melt Compositions to 330 °C With Application to Heat Flow and Geochemistry of the Ocean Crust: Journal of Geophysical Research: Solid Earth, v. 125, p. 1–20, doi:10.1029/2019JB017654.

Marks, M.A.W., Hettmann, K., Schilling, J., Frost, B.R., and Markl, G., 2011, The mineralogical diversity of alkaline igneous rocks: Critical factors for the transition from miaskitic to agpaitic phase assemblages: Journal of Petrology, v. 52, p. 439–455, doi:10.1093/petrology/egq086.

Marks, M.A.W., and Markl, G., 2017, A global review on agpaitic rocks: Earth-Science Reviews, v. 173, p. 229–258, doi:10.1016/j.earscirev.2017.06.002.

Meert, J.G., and Santosh, M., 2017, The Columbia supercontinent revisited: Gondwana Research, v. 50, p. 67–83, doi:10.1016/j.gr.2017.04.011.

Parmigiani, A., Degruyter, W., Leclaire, S., Huber, C., and Bachmann, O., 2017, The mechanics of shallow magma reservoir outgassing: Geochemistry, Geophysics, Geosystems, v. 18, p. 2887–2905, doi:10.1002/2017GC006912.

Pearce, N.J.G., 1988, The Petrology and Geochemistry of the Igaliko Dyke Swarm, South Greenland [PhD thesis], http://etheses.dur.ac.uk/6661/.

Piper, J.D.A., Thomas, D.N., Share, S., and Rui, Z.Q., 1999, The palaeomagnetism of (Mesoproterozoic) Eriksfjord group red beds, South Greenland: Multiphase remagnetization during the Gardar and Grenville episodes: Geophysical Journal International, v. 136, p. 739–756, doi:10.1046/j.1365-246X.1999.00756.x.

Salvi, S., and Williams-Jones, A.E., 1996, The role of hydrothermal processes in concentrating high-field strength elements in the Strange Lake peralkaline complex, northeastern Canada: Geochimica et Cosmochimica Acta, v. 60, p. 1917–1932, doi:10.1016/0016-7037(96)00071-3.

Scaillet, B., and Macdonald, R., 2004, Fluorite stability in silicic magmas: Contributions to Mineralogy and Petrology 2004 147:3, v. 147, p. 319–329, doi:10.1007/S00410-004-0559-1.

Sindern, S., and Kramm, U., 2000, Volume characteristics and element transfer of fenite aureoles: A case study from the Iivaara alkaline complex, Finland: Lithos, v. 51, p. 75–93, doi:10.1016/S0024-4937(99)00075-4.

Upton, B.G.J., 2013, Tectono-magmatic evolution of the younger Gardar southern rift, South Greenland (A. A. Garde, Ed.): Geol. Surv. Den. Green. Bull., v. 29, 1–128 p., doi:10.34194/geusb.v29.4692.

van de Ven, M.A.J., Borst, A.M., Davies, G.R., Hunt, E.J., and Finch, A.A., 2019, Hydrothermal Alteration of Eudialyte-Hosted Critical Metal Deposits: Fluid Source and Implications for Deposit Grade: Minerals, v. 9, p. 422, doi:10.3390/min9070422.

Woolley, A.R., Symes, R.F., and Elliott, C.J., 1972, Metasomatized (fenitized) quartzites from the Borralan Complex, Scotland: Mineralogical Magazine, v. 38, p. 819–836, doi:10.1180/minmag.1972.038.299.06.

Yan, P., Andersson, M., Kalscheuer, T., García Juanatey, M.A., Malehmir, A., Shan, C., Pedersen, L.B., and Almqvist, B.S.G., 2016, 3D magnetotelluric modelling of the Alnö alkaline and carbonatite ring complex, central Sweden: Tectonophysics, v. 679, p. 218–234, doi:10.1016/j.tecto.2016.05.002.

Zhou, B., Li, Z., and Chen, C., 2017, Global potential of rare earth resources and rare earth demand from clean technologies: Minerals, v. 7, p. 203, doi:10.3390/min7110203.

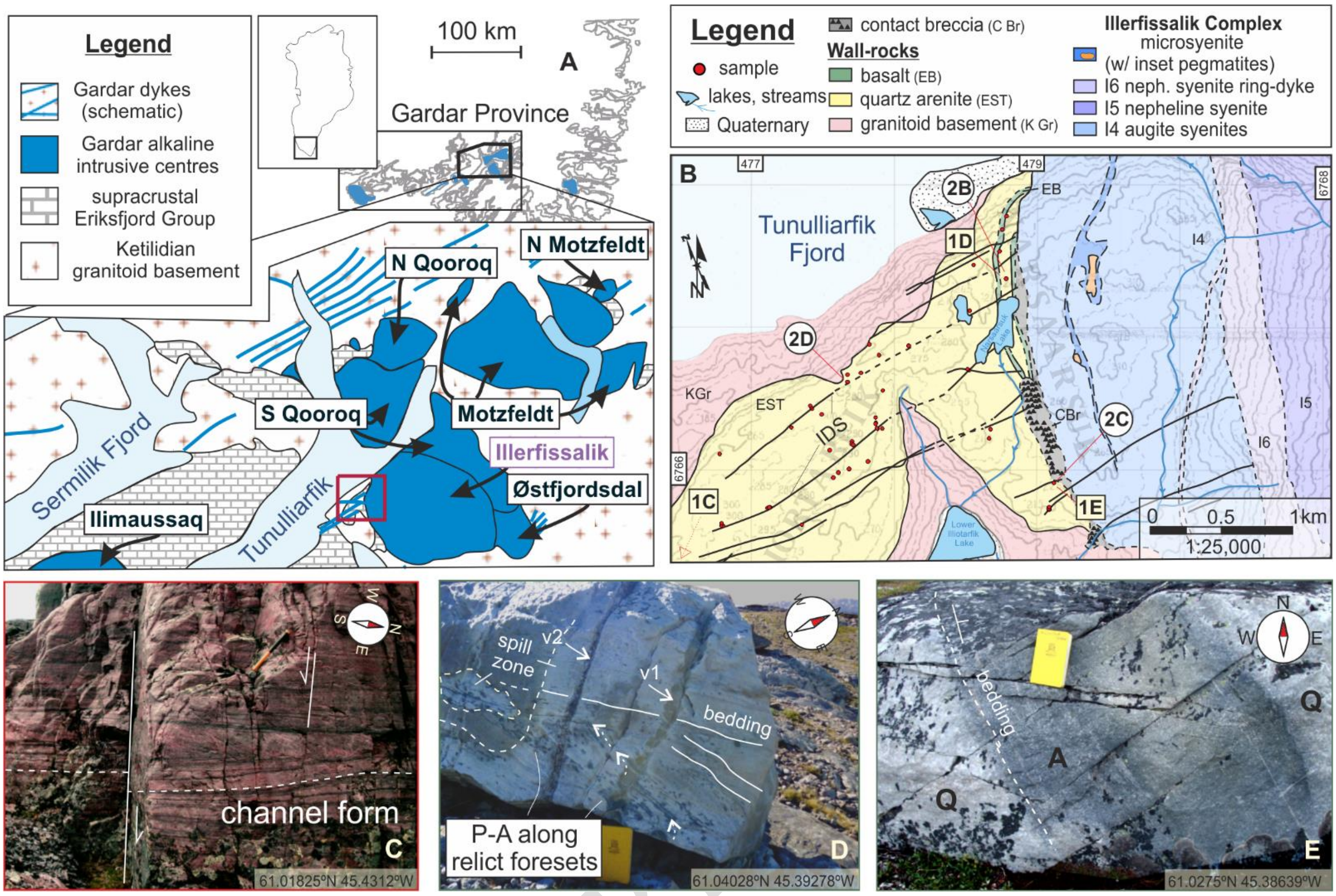

Figure 1. A) geological setting of the 'Igaliko Nepheline Syenite Complex' and its individual centres within the NE Gardar Province (modified after Garde et al., 2002; Ladenburger et al., 2016), study area extent shown in red; B) composite geological map (after Emeleus & Harry, 1970; Pearce, 1988; Upton, 2013) of the Illerfissalik Complex W margin, IDS = Igaliku Dyke Swarm, enclosed symbols denote locality photos (squares) and positions of fenite samples used on isocon plots in Fig.2 (circles), UTM grid Zone 23N; C) unaltered braided fluvial Eriksfjord Group protolith, SSW Illiortarfik, D-E) quartz(Q)-perthite-amphibole(A) fenite at N and S Narsaarsuk respectively with multiple penetrating vein generations (v1 – altered and eroded, v2 – fresher, intact) indicating likelihood of multiple alteration events

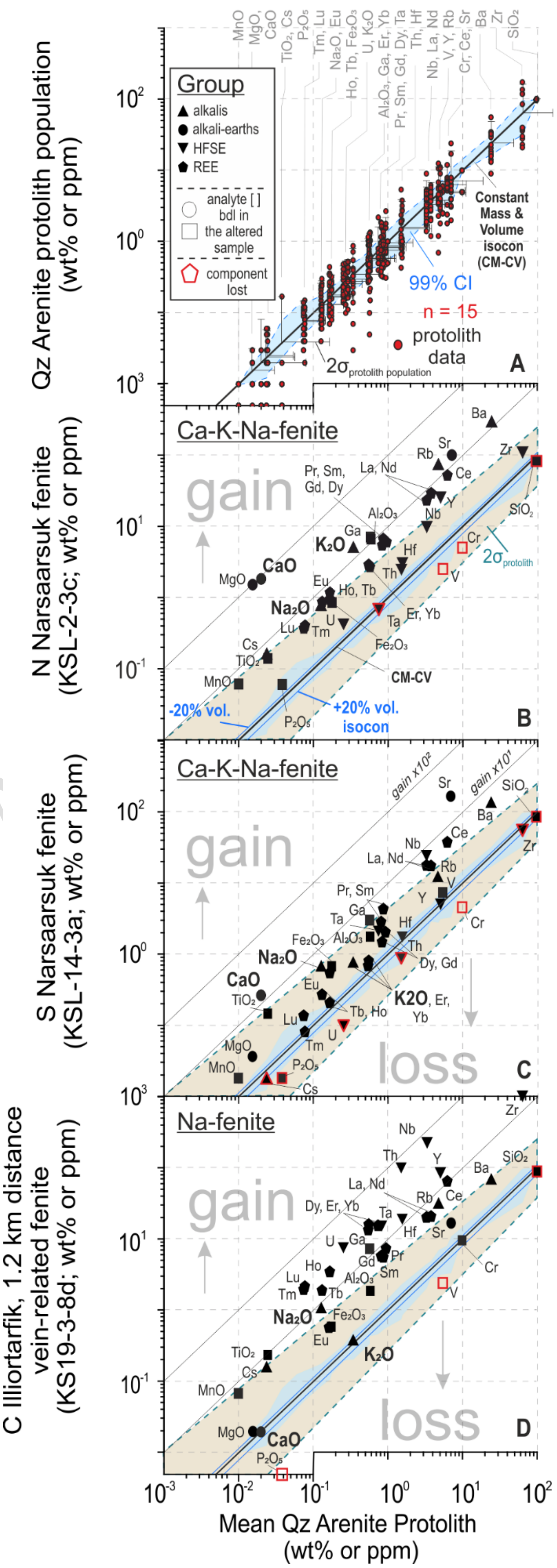

Figure 2. Constant mass isocon diagrams (after Grant, 1986) showing the mass-balance results; (A) distribution of the protolith sample population and 2σ deviation from the mean composition (error bars), (B-C) elemental gain-loss showing relatively intense (tenfold gain) alteration in the N Narsaarsuk fenite, less intense at S Narsaarsuk, and the distinct sodic nature of the fenite around late-stage veins beside an Igaliku dyke >1 km from Illerfissalik (D), major Ca-Na-K oxides defining alteration character emboldened, sample locations as in Fig. 1B; blue volume change lines plotted based on C_{SiO2} at f_v = 0.8-1.2

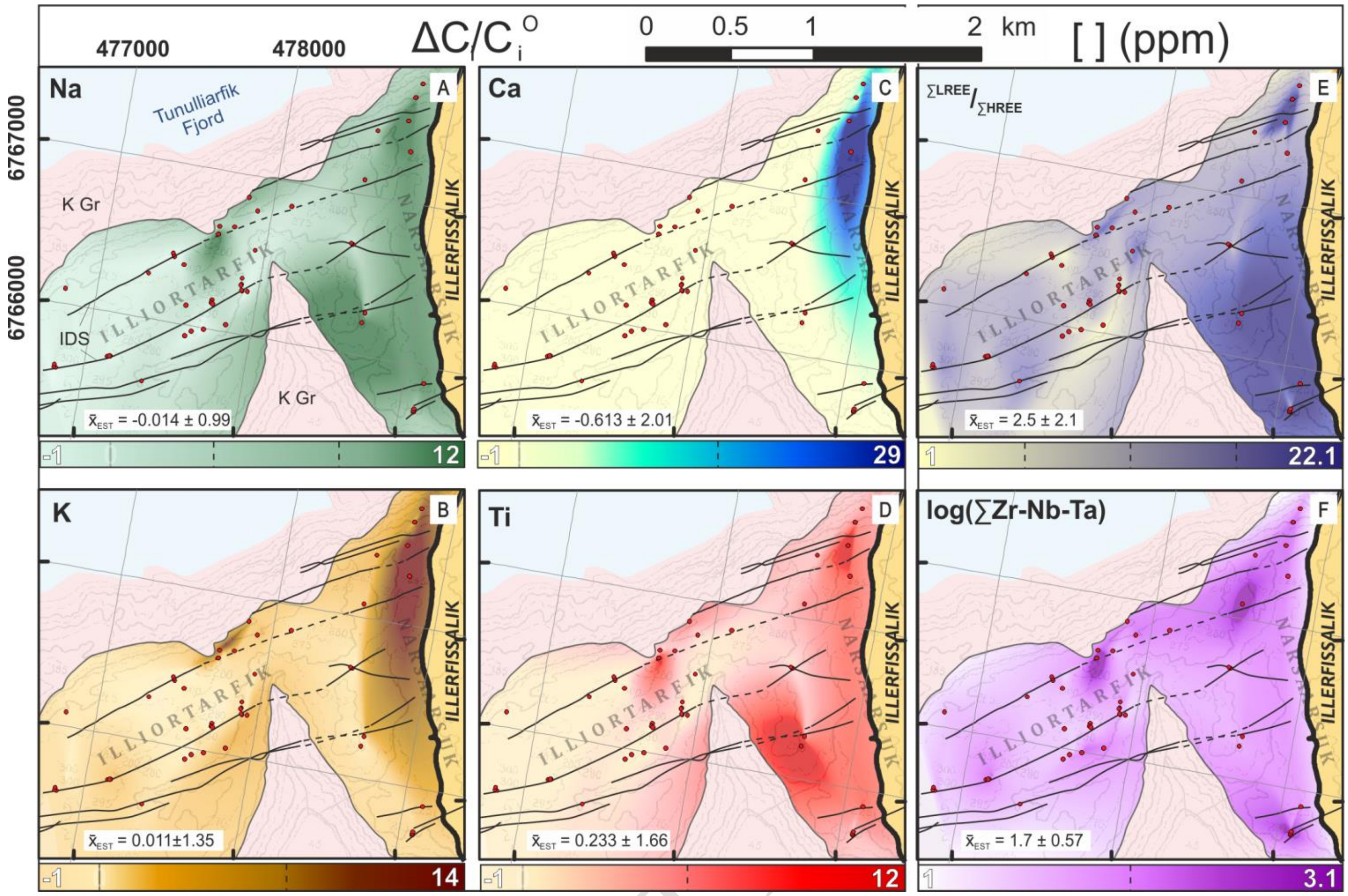

Figure 3. Spatial element maps showing intense Ca-K-Na fenitisation in the ~400 m wide zone by the Illerfissalik W margin particularly strong towards N Narsaarsuk with Zr-Nb-Ta-Ti excursions at further distance; created in ArcMap 10.7 using the Nearest Neighbour interpolation (output cell size = 1.4; sigmoid rendering used to accentuate midtones, strength 6, stretch-type colour ramp) of the isocon mass-balance $\Delta C_i/C_i^O$results (A-D), and the HFSE-REE raw data (E-F); ΣLREE = La-Gd, ΣHREE = Tb-Lu+Y; $\bar{x}_{EST}$ – parameter mean for the unaltered protolith population, error quoted at 2σ level; unit labels as in Fig. 1B

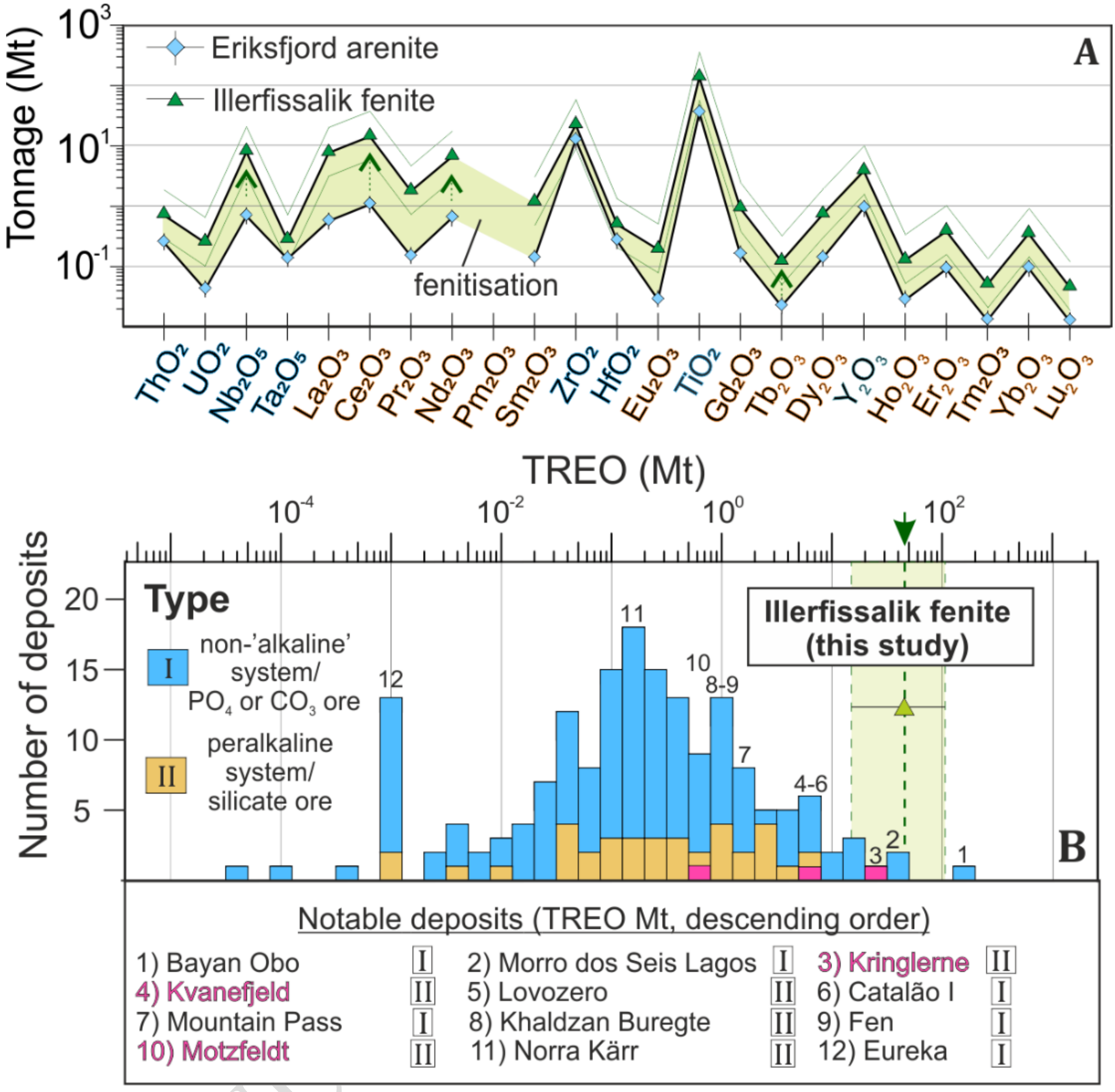

Figure 4. A) enrichment (~1 order of magnitude for Nb-LREE, lesser for other components) in the budget of individual HFSE oxides due to fenitization of the Eriksfjord protolith by the Illerfissalik fluids; non-lanthanides highlighted in blue on the x-axis; error bars for Eriksfjord cover only the range of three different geometries, max-min lines for fenite (pale-green range) denoting 0.2-0.8 km range of modelled fenite widths (see Fig. DR1.3C, Table DR2.6), see Supplementary Material DR1 for more detail

B) histogram of estimated mass (mean ~43 Mt, min-max defined by the range of results in iterated intrusion & fenite models, see Supplement DR1 and Tables DR2.2-2.5 for more detail) of the total rare-earth-oxides (TREO) stored within the Illerfissalik fenite, comparable to the tonnages hosted in many world-class type I and II magmatic-hydrothermal REE-ore deposits (Zhou et al., 2017; Greenlandic prospects shown in pink)